2016

# The role of a conserved membrane proximal cysteine in altering αPS2CβPS integrin diffusion

Aleem Syed
*Iowa State University*

Neha Arora
*Iowa State University*

Thomas A. Bunch
*University of Arizona*

Emily A. Smith
*Iowa State University*, esmith1@iastate.edu

# The role of a conserved membrane proximal cysteine in altering αPS2CβPS integrin diffusion

**Abstract**

Cysteine residues (Cys) in the membrane proximal region are common post-translational modification (PTM) sites in transmembrane proteins. Herein, the effects of a highly conserved membrane proximal *α*-subunit Cys1368 on the diffusion properties of *α*PS2C*β*PS integrins are reported. Sequence alignment shows that this cysteine is palmitoylated in human *α*3 and *α*6 integrin subunits. Replacing Cys1368 in wild-type integrins with valine (Val1368) putatively blocks a PTM site and alters integrins' ligand binding and diffusion characteristics. Both fluorescence recovery after photobleaching (FRAP) and single particle tracking (SPT) diffusion measurements show Val1368 integrins are more mobile compared to wild-type integrins. Approximately 33% and 8% more Val1368 integrins are mobile as measured by FRAP and SPT, respectively. The mobile Val1368 integrins also exhibit less time-dependent diffusion, as measured by FRAP. Tandem mass spectrometry data suggest that Cys1368 contains a redox or palmitoylation PTM in *α*PS2C*β*PS integrins. This membrane proximal Cys may play an important role in the diffusion of other alpha subunits that contain this conserved residue.

**Keywords**

Fluorescence recovery after photobleaching, Single particle tracking, Membrane protein biophysics, Receptor mobile fraction, Post-translational modification

**Disciplines**

Biology and Biomimetic Materials | Medicinal-Pharmaceutical Chemistry | Polymer and Organic Materials

**Comments**

This is an author-created, un-copyedited version of an article accepted for publication/published in *Physical Biology*. IOP Publishing Ltd is not responsible for any errors or omissions in this version of the manuscript or any version derived from it. The Version of Record is available online at DOI: 10.1088/1478-3975/13/6/066005. Posted with permission.

Physical Biology

OFFICIAL JOURNAL OF
Sociedad de Biofísicos Latino Americanos

PAPER

# The role of a conserved membrane proximal cysteine in altering $\alpha$PS2C$\beta$PS integrin diffusion

To cite this article: Aleem Syed *et al* 2016 *Phys. Biol.* **13** 066005

# The Role of a Conserved Membrane Proximal Cysteine in Altering αPS2CβPS Integrin Diffusion

*Aleem Syed[1], Neha Arora[1], Thomas A. Bunch[2] and Emily A. Smith[1,]**

*[1]Department of Chemistry, Iowa State University, 1605 Gilman Hall, Ames, Iowa 50011*

*[2]Cellular and Molecular Medicine, University of Arizona, Tucson, AZ 85721*

**esmith1@iastate.edu, (+1) 515-294-1424 (P), (+1) 515-294-0105(F)*

**Abstract**

Cysteine residues (Cys) in the membrane proximal region are common post-translational modification (PTM) sites in transmembrane proteins. Herein, the effects of a highly conserved membrane proximal α-subunit $Cys^{1368}$ on the diffusion properties of αPS2CβPS integrins are reported. Sequence alignment shows that this cysteine is palmitoylated in human α3 and α6 subunits. Replacing $Cys^{1368}$ with valine ($Val^{1368}$) putatively blocks a PTM site and alters integrins' ligand binding and diffusion characteristics. Both fluorescence recovery after photobleaching (FRAP) and single particle tracking (SPT) diffusion measurements show $Val^{1368}$ integrins are more mobile compared to $Cys^{1368}$ integrins. Approximately 33% and 8% more $Val^{1368}$ integrins are mobile as measured by FRAP and SPT, respectively. The mobile $Val^{1368}$ integrins also exhibit less time-dependent diffusion, as measured by FRAP. Tandem mass spectrometry data suggest that $Cys^{1368}$ contains a redox or palmitoylation PTM in αPS2CβPS integrins. This membrane proximal Cys may play an important role in the diffusion of other alpha subunits that bear this conserved residue.

**Key Words**

Fluorescence recovery after photobleaching

Single particle tracking

Membrane protein biophysics

Receptor mobile fraction

Post-translational modification

## 1. Introduction

The integrin family of cell surface receptors plays a critical role in many fundamental cellular processes like cell adhesion, progression, growth, and proliferation [1]. Integrins mediate bidirectional signaling across the cell membrane [2]. This signaling occurs via ligand binding to integrins (*outside-in signaling*) and via binding of several cytosolic proteins (*inside-out signaling*). In general, signaling depends on the concentration of the involved proteins and also their correct localization in the signaling region [3]. Recent studies highlighted the importance of post-translational modifications (PTM) in localizing a protein into membranes and membrane domains [4]. The goal of the current study is to identify the role of a highly conserved membrane proximal cysteine ($Cys^{1368}$) of the αPS2CβPS integrins on the receptor's lateral diffusion in the cell membrane.

Due to the nucleophilicity and redox sensitivity of non-disulfide cysteine amino acid residues, they are prone to various PTMs [5, 6]. Cysteine residues are modified through both spontaneous and enzyme-catalyzed reactions. Some of the common modifications include oxidation (*e.g.*, sulfhydration, glutathionylation, sulfenylation, sulfonation, and nitrosation), prenylation, palmitoylation, and Michael addition with lipid-derived electrophiles [7-11]. In addition to these, there are rare modifications at cysteine such as methylation and phosphorylation that are reported for both eukaryotic and prokaryotic proteins [12]. There are diverse functional consequences on protein localization, interactions, and trafficking in the cell membrane as a result of cysteine PTMs [13]. Alterations in cysteine PTMs are reported to contribute to proliferative and degenerative diseases [14-16].

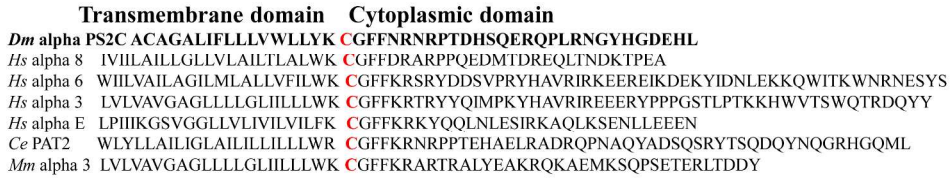


**Figure 1.** Sequence alignment of integrin's α-cytoplasmic and transmembrane domains across different species. The single-letter amino acid code is used. Species are: *Ce*, *Caenorhabditis elegans*; *Dm*, *Drosophila melanogaster*; *Hs*, *Homo sapiens*; *Mm, Mus musculus*. The amino acid sequence of *Drosophila* αPS2C domain is shown in bold and the conserved cysteines are shown in red.

Figure 1 depicts the multiple sequence alignment of the transmembrane and cytoplasmic domains of selected integrin α subunits of *Caenorhabditis elegans, Drosophila melanogaster*, *Homo sapiens, and Mus musculus*. There is a cysteine in the membrane proximal region that is conserved among all the subunits. This specific cysteine is palmitoylated in human α3 and α6 integrin subunits [17]. Palmitoylation increases the affinity of proteins towards membranes nanodomains [18]. This leads to the hypothesis that the highly conserved cysteine in the membrane proximal region of αPS2CβPS integrins and its putative PTMs play a role in governing the receptor's biophysical properties. Additionally, it has been reported that the highly conserved GFFXR domain adjacent to the cysteine regulates the adhesive and ligand binding properties of integrins. The deletion of the cytoplasmic tail after the GFFXR domain, deleting the GFFXR domain, or mutating the GFFXR sequence resulted in a two to twelve-fold *increase* in ligand binding affinity compared to wild-type human and *Drosophila* integrins in several cell types [19-22]. On the other hand, there was a two-fold *decrease* in ligand binding affinity when $Cys^{1368}$ is replaced with $Val^{1368}$ in the α subunit of αPS2CβPS integrins [23]. If $Cys^{1368}$ alters αPS2CβPS integrin diffusion properties, it is expected that a mutation to a different residue at

this position will produce altered diffusion properties compared to the wild-type receptor. We test this hypothesis by generating a $Val^{1368}$ mutation through site directed mutagenesis. The consequences of this mutation on integrin diffusion are measured using fluorescence microscopy. Ensemble diffusion, that is an average across numerous receptors, is measured using fluorescence recovery after photobleaching (FRAP) and the diffusion of single receptors is measured using single particle tracking (SPT). Since receptor diffusion is primarily non-synchronous, measuring one receptor at a time accounts for diffusion heterogeneity. Finally, tandem mass spectrometry is used to identify potential PTMs at $Cys^{1368}$.

## 2. Material and Methods

### *2.1. Cell culture*

*Drosophila* S2 cells were grown in Shields and Sang M3 insect media (M3, Sigma) supplemented with 10% fetal bovine serum (Irvine Scientific), 12.5 mM streptomycin, 36.5 mM penicillin, and 0.2 μM methotrexate (Fisher Scientific). Six stably transformed S2 cell lines were developed by expressing: (i) wild-type (αPS2CβPS) integrins, (ii) $Val^{1368}$ (αPS2C(C1368V)βPS) integrins, (iii) Venus yellow fluorescent protein (YFP)-tagged wild-type integrins, (iv) YFP-tagged $Val^{1368}$ integrins, (v) HA (YPYDVPDYA)-tagged wild-type integrins, and (vi) HA-tagged $Val^{1368}$ integrins. YFP or HA tags were inserted in the 40-amino-acid extracellular serine-rich loop. The extracellular serine-rich loop has been used previously to insert epitope tags with minimum perturbation to integrin functions, such as ligand binding [24, 25]. The heat shock inducible promoter was used to express all exogenous proteins. Cells were maintained in a 22°C incubator and were heat-shocked in a 36 °C water bath for 30 min to induce expression of integrins before conducting any further experiments.

*2.2. Immunoprecipitation and LC-MS/MS analysis of wild-type and Val$^{1368}$ integrins*

Both wild-type and Val$^{1368}$ integrin alpha subunits were purified using an HA (YPYDVPDYA) epitope tag. S2 cells expressing HA-tagged wild-type or Val$^{1368}$ integrins were heat-shocked for 30 minutes in a 36 °C water bath. Cells were kept in a 22 °C incubator for 3 hours before cell lysis. Cells were lysed using RIPA buffer (150 mM sodium chloride, 1.0% NP-40 detergent, 0.5% sodium deoxycholate, 0.1% sodium dodecyl sulfate, 50 mM Tris, pH8.0) as described previously [26]. Cell lysates were incubated with Pierce™ anti-HA magnetic beads using the manufacturer's instructions. Bound HA-tagged wild-type or Val$^{1368}$ integrin alpha subunit was eluted by incubating the beads at 95 ºC for 10 minutes with sodium dodecyl sulfate sample buffer (5% SDS, 5% Glycerol, 125 mM Tris-HCl (pH=6.8) and 0.01% Bromophenol Blue). Supernatant from the elution step was directly added to a pre-cast protein gel for separation by electrophoresis. Coomassie stained protein bands corresponding to wild-type or Val$^{1368}$ integrin alpha subunit were excised from the gel and were digested with trypsin or chymotrypsin on an automated ProGest (Digilab, Marlborough, MA) protein digestion station. Digested fragments were loaded onto the Q-Exactive tandem mass spectrometer (Thermo Scientific) for LC-MS/MS analysis. The measured peptide fragments were searched for potential PTMs including sulfhydration (addition of –SH), nitrosation (addition of –NO), sulfonation (addition of -$SO_3$) and palmitoylation (addition of palmitic acid through acylation of thiol on cysteine).

*2.3. Instrumentation*

A Nikon Eclipse TE2000U microscope (Melville, NY, USA) equipped with an oil immersion objective (100×, 1.49 NA) was used for all microscopy experiments. A mercury lamp was used for imaging, and fluorescence images were collected using a PhotonMAX 512 EMCCD camera (Princeton Instrument, Trenton, NJ, USA). For SPT, a filter set from Omega Optical (XF304-1, Brattleboro, VT, USA) was used for excitation (425/45-nm) and to collect the quantum dot

emission (605/20-nm). FRAP images were collected using a 500/20-nm excitation and a 535/30-nm emission filter.

*2.4. FRAP microscopy*

FRAP data were collected and analyzed according to previously published protocols [26-28]. Briefly, cells expressing YFP-tagged wild-type or $Val^{1368}$ integrins were plated onto ligand-coated glass slides. A series of images were acquired before and after photobleaching using mercury-lamp excitation on a timeframe of 75 s. Photobleaching was accomplished with the 488-nm line of an argon ion laser. Data were analyzed using ImageJ version 1.38. FRAP curves were fit to extract diffusion parameters according to the method of Feder *et al.* by fitting the recovery curves to three different models - Brownian, constrained, and mixed diffusion [29]. A reduced $chi^2$ value closest to 1 was used to indicate the best-fit model, which was the mixed diffusion model for all presented data.

*2.5. Single particle tracking*

Amine-derivatized polyethylene glycol (PEG) quantum dots (Life Technologies) measuring 16-nm in diameter and with emission maxima at 605-nm were used for SPT measurements. Quantum dot probes for SPT were prepared as previously reported [27]. Briefly, quantum dots were conjugated with a recombinant version of the αPS2CβPS integrin ligand, RBB-tiggrin, by mixing a ratio of 1 quantum dot to 20 RBB-Tiggrin in 10 mM phosphate buffer, pH 8.5 for 2 h. The ligand-coated quantum dots were sonicated for 2 h before diluting to the required concentration for cell incubation, and were then used within half an hour to limit the aggregation of quantum dots [27].

Quantum dot-labeled integrins were localized and tracked using the Particle Tracker Plugin of ImageJ. A total of 91 trajectories were generated for each cell line. Data analysis was performed using a graphical user interface (GUI) in MATLAB to distinguish trajectories with

Brownian diffusion, confined diffusion, to calculate diffusion coefficients, and to identify immobile integrin fractions [30]. Only a small fraction of the total integrins in the cell membrane are measured in an SPT experiment. This is necessary to reduce the possibility that two or more QDs are colocalized within the diffraction volume, which would prohibit localizing and tracking each individual QD.

## 3. Results and Discussion

### *3.1. $Cys^{1368}$ to $Val^{1368}$ mutation increases αPS2CβPS integrins' mobile fraction*

S2 cells expressing wild-type $Cys^{1368}$ integrins or $Val^{1368}$ integrins are used in this study to reveal the role of $Cys^{1368}$ in altering the receptor's diffusion properties. Table 1 lists the diffusion parameters for both cell lines obtained from the FRAP curves shown in figure 2. The percentage of mobile wild-type integrins is 59.9 ± 0.7% as measured by FRAP. In comparison, 93 ± 1% of the integrins are mobile in cells expressing $Val^{1368}$ integrins. Similar to the FRAP results, SPT also measured more mobile integrin trajectories in the $Val^{1368}$ cell line (80%) compared to the wild-type cell line (72%) as shown in table 2. (The values measured by SPT are obtained from counting among all measured trajectories so no uncertainty reported). The percent mobile fraction measured by FRAP and the percent mobile trajectories measured by SPT are not necessarily comparable due to the nature of the measurements, as further outlined below. However, the trend between the wild-type and $Val^{1368}$ integrin mobile fraction measured by FRAP and the trend between the wild-type and $Val^{1368}$ integrin mobile trajectories measured by SPT reveal the presence of $Cys^{1368}$ results in the immobilization of a fraction of integrins.

**Table 1.** Diffusion parameters obtained from FRAP experiments.

| | D (1s) ($\mu m^2/s$)[1] | α | Mobile fraction (%) |
|---|---|---|---|
| **Wild-type integrins** | 0.69 ± 0.02 | 0.59 ± 0.01 | 59.9 ± 0.7 |
| **$Val^{1368}$ integrins** | 0.52 ± 0.02 | 0.74 ± 0.02 | 93 ± 1 |

[1]The uncertainty in the diffusion parameters represents one standard deviation in fitting the average FRAP curves from at least 10 replicate measurements. There are other experimental uncertainties, such as the excitation volume from the laser profile, that have not been included in these uncertainties and which will increase the uncertainty.

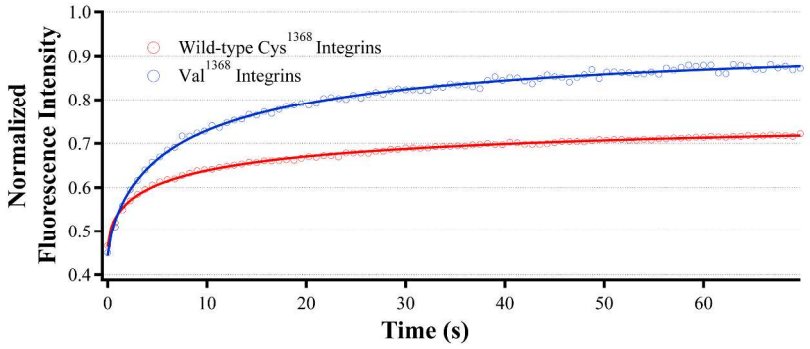


**Figure 2.** Average fluorescence recovery after photobleaching (FRAP) curves (open circles) and corresponding best fit (solid line) to the data. The diffusion parameters extracted from the fit are shown in table 1.

**Table 2.** Diffusion parameters obtained from SPT experiments.

| | Wild-type integrins | $Val^{1368}$ integrins |
|---|---|---|
| **Total Mobile trajectories (%)** | 72 | 80 |
| **Average diffusion coefficient for Brownian trajectories ($\mu m^2/s$)** | 0.27 | 0.10 (p=0.22) |
| **Number of confined domains in 30 seconds** | 3 | 3 |
| **Average diffusion coefficient inside the confined domains ($\mu m^2/s$)** | 0.013 | 0.031 (p=0.29) |
| **Average time in confined domains (s)** | 2.36 | 2.44 (p=0.57) |
| **Average diameter of the Confined domains ($\mu m$)** | 0.260 | 0.370 (p=0.16) |

p values are obtained from comparing wild-type and $Val^{1368}$ data sets using the Kolmogorov–Smirnov (K-S) test.

A difference between the FRAP and SPT experiments is the population of integrins that are measured. All integrins with a fluorescent tag, that is all the integrins in these FRAP studies, contribute to the FRAP signal. On the other hand, the integrins must be bound to ligand on the quantum dot in order to generate a signal in SPT. This may explain the difference in the percentage change of the mobile fraction as measured by the two techniques. In other words, there is a smaller increase in the mobile fraction of the ligand-bound population of integrins measured by SPT as compared with the total integrin population as measured by FRAP when $Cys^{1368}$ is replaced with $Val^{1368}$. In addition, the mobile fraction measured in FRAP requires the receptor to diffuse outside of a region defined by the dimensions of the laser beam (diameter of 5.72 μm) whereas, the mobile trajectories in SPT only need to move a distance greater than the positional uncertainty in localizing the nanoparticle (0.014 μm).

*3.2. $Cys^{1368}$ to $Val^{1368}$ mutation generates more Brownian-like diffusion as measured by FRAP*

The α value measured by FRAP is indicative of the time dependence of the diffusion coefficient. An α value of 1 represents Brownian diffusion; lower α values are indicative of more diffusion constraints and a time-dependent diffusion coefficient. For wild-type integrins, the measured α was 0.59 ± 0.01 and this increased to 0.74 ± 0.02 with $Val^{1368}$ mutation, indicating more Brownian-like diffusion for $Val^{1368}$ integrins. The local constraints to the diffusion of membrane protein arise from interaction with other intracellular, membrane or extracellular components. The $Val^{1368}$ mutation may alter one or a combination of interactions, resulting in less time-dependent diffusion.

As measured by SPT, confined domains are defined as regions in the cell membrane where a receptor is located for a time period that is longer than can be explained by Brownian diffusion. Diffusion is Brownian when no confined domains exist during the observed trajectory. A confinement index, L, was calculated at each time point of each trajectory. An L greater than 3.16 for a duration greater than 1.125 s had a likelihood of greater than 99% to reflect confined diffusion as determined from simulated data [26]. Figure 3 shows trajectories and plots of the confinement index and diffusion coefficient for a trajectory exhibiting only Brownian diffusion and a trajectory with one confined domain (blue circle). As expected, the confinement index and diffusion coefficient are inversely proportional.

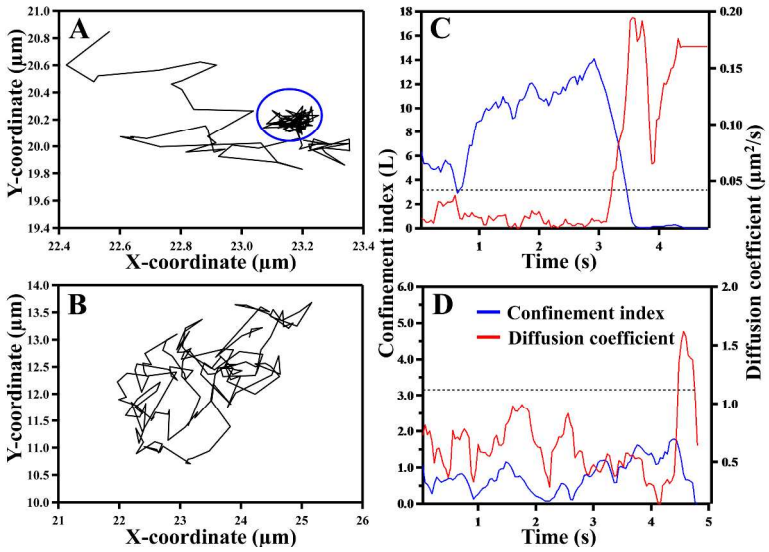


**Figure 3.** Plots showing (A) a trajectory with a single confined domain depicted by a blue circle; (B) a Brownian trajectory with no confined domains. Right panel C-D shows instantaneous diffusion coefficient and confinement index plots. Confined domains are identified from the calculated confinement index (L). An L greater than 3.16 (shown by the dotted line in C and D) for a duration greater than 1.125 s has a greater than 99% likelihood to reflect confined diffusion.

There is no significant difference in the number of confined domains measured for wild-type and $Val^{1368}$ integrins (3 confined domains per 30 seconds). When a trajectory shows regions of confinement, the trajectory is further analyzed to determine the size of the confined domains, time in the confined domains and the diffusion coefficient inside the confined domains. These parameters are calculated and compared between wild-type and $Val^{1368}$ integrins (table 2). Frequency histograms of confined domain size and duration of confinement are shown in figures 4 and 5, respectively. For wild-type integrins, confined domains are 0.260-µm in diameter and the confinement lasted for an average of 2.36 s. There is no statistically significant change in either the time in (2.44 s) or diameter of (0.370-µm) confined domains measured for $Val^{1368}$ integrins. While there is no statistically significant change in the average domain size, it is worthy to note that the largest domain size measured for wild-type integrins is 0.896-µm, while the largest

measured for Val$^{1368}$ integrins is 2.520-μm.

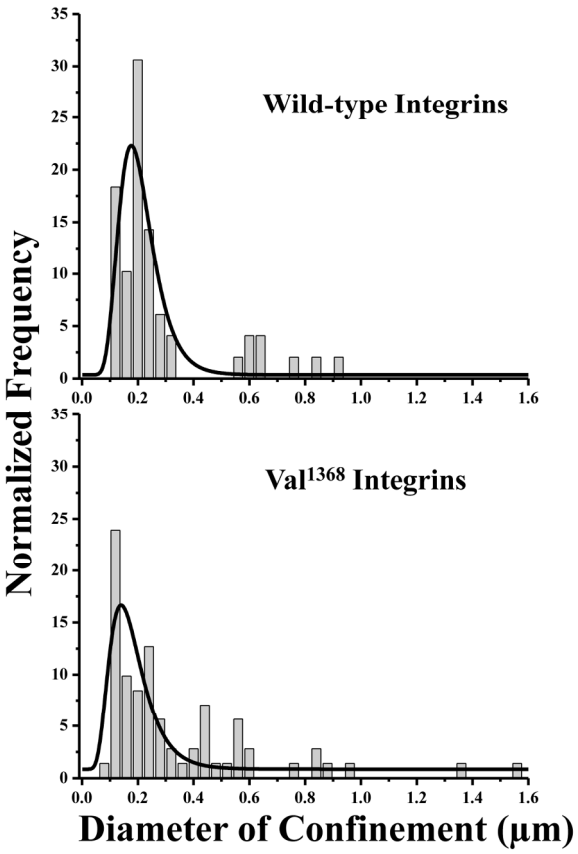


**Figure 4.** Frequency histograms of the size of confined domains. The results were normalized to the total number of measured confined domains (wild-type: 49 confined domains over 539 seconds, and Val$^{1368}$ mutant: 71 confined domains over 723 seconds). For clarity, two values are omitted from the Val$^{1368}$ graph: one at 2.52 μm and one at 2.08 μm.

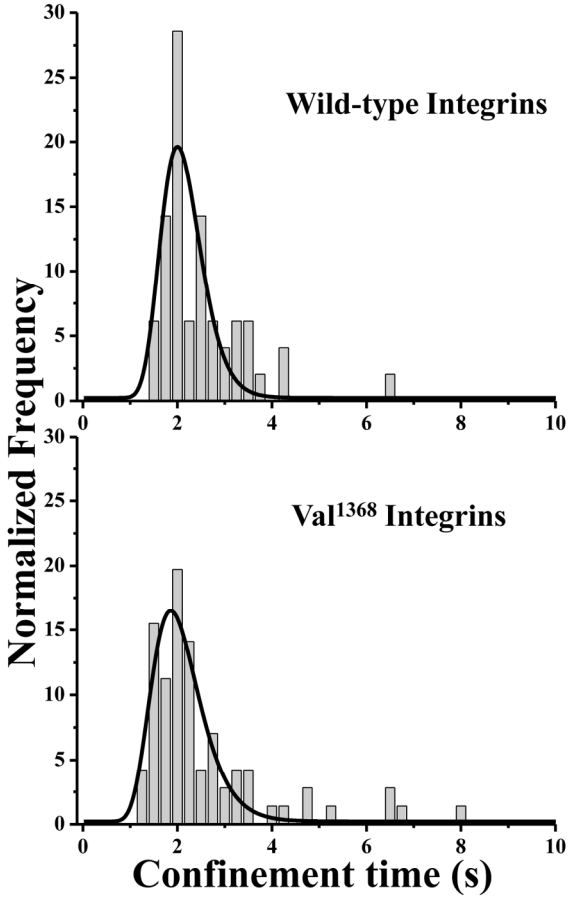


**Figure 5.** Frequency histograms of the duration of confined domains. The results were normalized to the total number of measured confined domains.

*3.3. Alterations in the diffusion coefficient after Cys$^{1368}$ to Val$^{1368}$ mutation*

The last diffusion property to consider is the diffusion coefficient. The average diffusion coefficient measured by FRAP at one second decreased 25% when Cys$^{1368}$ in wild-type integrins is replaced with Val$^{1368}$. As discussed above, the diffusion coefficient is time dependent as a result of $\alpha$ being less than one; the percent difference in the diffusion coefficient is also time dependent.

For SPT data, an average diffusion coefficient from all points in the trajectory is

calculated for the Brownian trajectories. Furthermore, the diffusion coefficients inside confined domains are separately calculated. As shown in table 2, the average diffusion coefficient of $Val^{1368}$ integrins was statistically similar to the average diffusion coefficient of wild-type integrins inside and outside confined domains (*i.e.*, when diffusion is Brownian). This indicates that $Cys^{1368}$ does not affect the average diffusion coefficient of the ligand-bound integrins as measured in SPT. There is a 4 order of magnitude spread (0.001 to 10 s) in diffusion coefficients measured by SPT, which is consistent with the high degree of diffusion coefficient heterogeneity for many receptors (figure 6).

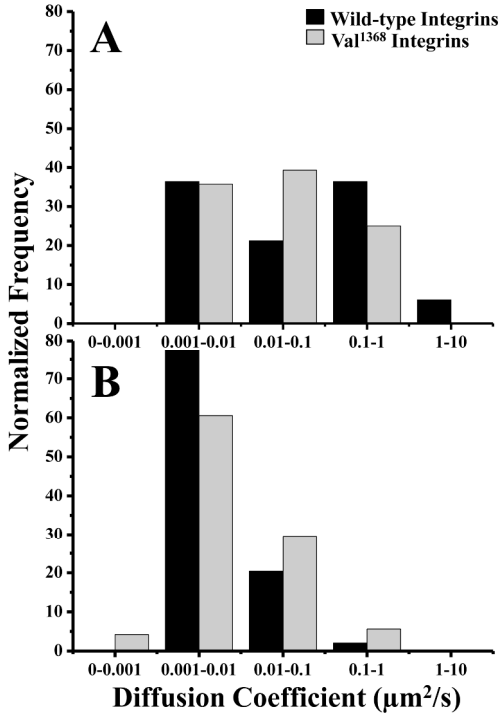


**Figure 6.** Histogram of diffusion coefficients of mobile wild-type and $Val^{1368}$ integrins exhibiting (A) Brownian diffusion and (B) for diffusion within confined domains. Histograms were normalized with respect to the total number of trajectories in each data set.

*3.4. Post-translational modification of Cys$^{1368}$*

Tandem mass spectrometry was used to identify modifications at Cys$^{1368}$ on the αPS2C subunit. Trypsin digestion of wild-type αPS2C unexpectedly did not result in detection of the peptide containing Cys$^{1368}$. Trypsin digests at lysine residues; in the case of the αPS2C subunit, there is a lysine adjacent to Cys$^{1368}$ at the C-terminus. Cleavage at this lysine should generate an easy to detect hydrophilic peptide. If trypsin does not cut at this adjacent lysine, however, the next nearest cut site is 36 amino acids away into the extracellular domain. This would generate a hard to detect, large hydrophobic peptide. Interestingly, the expected fragment containing Val$^{1368}$ was detected after trypsin digestion (table 3), indicating the specific presence of Cys$^{1368}$ prevents trypsin digestion. We hypothesize that a PTM at Cys$^{1368}$ inhibits trypsin digestion (possibly due to steric hindrance) at the adjacent lysine. Peptides containing palmitoylated cysteine (Cys$^{104}$ and Cys$^{170}$) were detected in the fragment mass spectrum, however, these were found in small hydrophilic peptides.

On the other hand, chymotrypsin digestion (primarily at tyrosine, phenylalanine, tryptophan, and to a lesser extent at leucine and methionine) of integrin αPS2C subunit does produce peptides containing Cys$^{1368}$. The mapped amino acids are shown in figure S1 in red font. The Cys$^{1368}$ is observed to be modified with a sulfhydryl group or a sulfo group in four detected peptides as shown in table 3. The peptides with sulfhydryl or sulfo-modified Cys$^{1368}$ are detected in four independent analyses, although the confidence match in the fragment mass spectrum was low. In two of the four analyses, peptides containing Cys$^{1368}$ are also observed to be nitrosylated (addition of –NO) as shown in table 3. It is reported that cysteine modification occurs through nitrosation, as direct sulfhydration is not energetically favorable [31]. Palmitoylation at Cys$^{1368}$, however, is not excluded based on the collected data. Detected palmitoylation sites measured after trypsin digestion produce the same PTM detected at Cys$^{1368}$ after chymotrypsin digestion. It is possible that palmitoylation is more labile in these chymotrypsin digests. In summary, redox PTMs were detected on Cys$^{1368}$. Given the sequence homology to other integrin alpha subunits

that are known to be palmitoylated at this site, it is highly suspected that Cys$^{1368}$ is palmitoylated in αPS2C.

**Table 3.** Identified peptide fragment containing **Cys$^{1368}$** or **Val$^{1368}$** and corresponding identified post-translational modification.

| Detected Peptides | Detected Post Translational Modification | $MH^+$ (Da) | m/z (Da) |
|---|---|---|---|
| **VGFFNR** | none | 739.39 | 370.20 |
| **KCGFFNRNRPTDHSQERQPL** | C2(Sulfo); R17(Deamidated) | 2511.13 | 1256.07 |
| **VWLLYKCGF** | C7(Sulfo) | 1208.54 | 604.78 |
| **LYKCGFFNRNRPTDHSQERQPLRNGYHGDEHL** | C4(Sulfo); N10(Deamidated); N24(Deamidated) | 3966.77 | 992.45 |
| **LLYKCGFFNRNRPTDHSQERQPL** | C5(Sulfo) | 2899.38 | 1450.19 |
| **LLYKCGF** | C5(Sulhydration) | 844.45 | 422.73 |
| **LYKCGFFNRNRPTDHSQERQPL** | C4(Sulhydration); N8(Deamidated); N10(Deamidated) | 2709.30 | 903.78 |
| **KCGFFNRNRPTDHSQERQPLRNGY** | C2(Sulhydration); R9(Deamidated); R17(Deamidated); R21(Deamidated) | 2924.37 | 975.46 |
| **LLYKCGFF** | C5(Sulhydration) | 991.52 | 496.26 |
| **YKCGFFNRNRPTDHSQERQPL** | C3(Nitrosyl); R8(Deamidated); R10(Deamidated); R18(Deamidated) | 2625.18 | 875.73 |
| **YKCGFFNRNRPTDHSQERQPLRNGY** | C3(Nitrosyl) | 3112.47 | 778.87 |

## 4. Conclusions

This study revealed a role of $Cys^{1368}$ in altering αPS2CβPS integrin diffusion. Both FRAP and SPT measured more mobile integrins when $Cys^{1368}$ is mutated, as well as less time-dependent diffusion and a slower average diffusion coefficient as measure by FRAP. $Cys^{1368}$ is proposed to be an important PTM site that regulates the diffusion properties of αPS2CβPS integrins; this conserved cysteine may play a similar role in the biophysical properties of the other integrins listed in figure 1.

## Conflict of Interest

Authors declare no conflict of interest.

## Acknowledgements

Support for this work was provided by the National Science Foundation (CHE-0845236 and CHE-1412084). The cell lines used in this study were developed by TAB with financial support from National Institutes of Health (R01GM42474). The authors thank Joel Nott of the protein facility at Iowa State University for help with mass spectrometry.

## 5. References


[1] F.G. Giancotti, E. Ruoslahti 1999 Integrin signaling *Science*, **285**, 1028-1032.

[2] J. Qin, O. Vinogradova, E.F. Plow 2004 Integrin bidirectional signaling: a molecular view *PLoS biology*, **2**, e169.

[3] J. Goedhart, J. van Unen, M.J.W. Adjobo-Hermans, T.W.J. Gadella 2013 Signaling efficiency of G alpha q through its effectors p63RhoGEF and GEFT depends on their subcellular location *Sci. Rep.*, **3**.

[4] M.J. Nadolski, M.E. Linder 2007 Protein lipidation *FEBS J.*, **274**, 5202-5210.

[5] R.K. Cannan, B.C. Knight 1927 Dissociation Constants of Cystine, Cysteine, Thioglycollic Acid and alpha-Thiolactic Acid *Biochem. J.*, **21**, 1384-1390.

[6] Z.R. Gan, W.W. Wells 1987 Identification and reactivity of the catalytic site of pig liver thioltransferase *J.Biol.Chem.*, **262**, 6704-6707.

[7] M. Lo Conte, K.S. Carroll 2013 The redox biochemistry of protein sulfenylation and sulfinylation *J. Biol.Chem.*, **288**, 26480-26488.

[8] N. Gould, P.T. Doulias, M. Tenopoulou, K. Raju, H. Ischiropoulos 2013 Regulation of protein function and signaling by reversible cysteine S-nitrosylation *J. Biol. Chem.*, **288**, 26473-26479.

[9] O. Kabil, N. Motl, R. Banerjee 2014 H2S and its role in redox signaling *Biochim. Biophys. Acta-Proteins and Proteomics*, **1844**, 1355-1366.

[10] F.L. Zhang, P.J. Casey 1996 Protein prenylation: molecular mechanisms and functional consequences *Annu. Rev. Biochem.*, **65**, 241-269.

[11] C.T. Tom, B.R. Martin 2013 Fat chance! Getting a grip on a slippery modification *ACS Chem. Biol.*, **8**, 46-57.

[12] S.M. Couvertier, Y. Zhou, E. Weerapana 2014 Chemical-proteomic strategies to investigate cysteine posttranslational modifications *Biochim. Biophys. Acta-Proteins and Proteomics*, **1844**, 2315-2330.

[13] J. Charollais, F.G. Van Der Goot 2009 Palmitoylation of membrane proteins (Review) *Mol. Membr. Biol.*, **26**, 55-66.

[14] A. Garcia-Garcia, L. Zavala-Flores, H. Rodriguez-Rocha, R. Franco 2012 Thiol-Redox Signaling, Dopaminergic Cell Death, and Parkinson's Disease *Antioxid. Redox Signal.*, **17**, 1764-1784.

[15] Y.M. Go, D.P. Jones 2011 Cysteine/cystine redox signaling in cardiovascular disease *Free Radic. Biol. Med.*, **50**, 495-509.

[16] M.D. Resh 2012 Targeting protein lipidation in disease *Trends Mol. Med.*, **18**, 206-214.

[17] X. Yang, O.V. Kovalenko, W. Tang, C. Claas, C.S. Stipp, M.E. Hemler 2004 Palmitoylation supports assembly and function of integrin-tetraspanin complexes *J. Cell Biol.*, **167**, 1231-1240.

[18] I. Levental, D. Lingwood, M. Grzybek, U. Coskun, K. Simons 2010 Palmitoylation regulates raft affinity for the majority of integral raft proteins *Proc. Natl. Acad. Sci. U.S.A.*, **107**, 22050-22054.

[19] T.A. Bunch, T.L. Helsten, T.L. Kendall, N. Shirahatti, D. Mahadevan, S.J. Shattil, D.L. Brower 2006 Amino acid changes in Drosophila alphaPS2betaPS integrins that affect ligand affinity *J. Biol. Chem.*, **281**, 5050-5057.

[20] P.E. Hughes, F. Diaz-Gonzalez, L. Leong, C. Wu, J.A. McDonald, S.J. Shattil, M.H. Ginsberg 1996 Breaking the integrin hinge. A defined structural constraint regulates integrin signaling *J. Biol. Chem.*, **271**, 6571-6574.

[21] T.E. O'Toole, Y. Katagiri, R.J. Faull, K. Peter, R. Tamura, V. Quaranta, J.C. Loftus, S.J. Shattil, M.H. Ginsberg 1994 Integrin cytoplasmic domains mediate inside-out signal transduction *J. Cell Biol.*, **124**, 1047-1059.

[22] C.F. Lu, T.A. Springer 1997 The alpha subunit cytoplasmic domain regulates the assembly and adhesiveness of integrin lymphocyte function-associated antigen-1 *J. Immunol.*, **159**, 268-278.

[23] T. Kendall, L. Mukai, A.L. Jannuzi, T.A. Bunch 2011 Identification of integrin beta subunit mutations that alter affinity for extracellular matrix ligand *J. Biol. Chem.*, **286**, 30981-30993.

[24] T.A. Bunch, T.L. Helsten, T.L. Kendall, N. Shirahatti, D. Mahadevan, S.J. Shattil, D.L. Brower 2005 Amino Acid Changes in Drosophila PS2betaPS Integrins That Affect Ligand Affinity *J. Biol. Chem.*, **281**, 5050-5057.

[25] T. Kendall, L. Mukai, A.L. Jannuzi, T.A. Bunch 2011 Identification of Integrin Subunit Mutations That Alter Affinity for Extracellular Matrix Ligand *J. Biol. Chem.*, **286**, 30981-30993.

[26] N. Arora, A. Syed, S. Sander, E.A. Smith 2014 Single particle tracking with sterol modulation reveals the cholesterol-mediated diffusion properties of integrin receptors *Phys. Biol.*, **11**, 066001.

[27] D. Mainali, E.A. Smith 2013 The effect of ligand affinity on integrins' lateral diffusion in cultured cells *Eur. Biophy. J.*, **42**, 281-290.

[28] S. Sander, N. Arora, E.A. Smith 2012 Elucidating the role of select cytoplasmic proteins in altering diffusion of integrin receptors *Anal. Bioanal. Chem.*, **403**, 2327-2337.

[29] T.J. Feder, I. Brust-Mascher, J.P. Slattery, B. Baird, W.W. Webb 1996 Constrained diffusion or immobile fraction on cell surfaces: a new interpretation *Biophys. J.*, **70**, 2767-2773.

[30] S.A. Menchon, M.G. Martin, C.G. Dotti 2012 APM_GUI: analyzing particle movement on the cell membrane and determining confinement *BMC Biophys.*, **5**, 4.

[31] M.R. Filipovic 2015 Persulfidation (S-sulfhydration) and H2S *Handb Exp. Pharmacol.*, **230**, 29-59.